Deposition of Disinfectant Poly(methyl acrylate) Nanocapsules onto Natural Rubber Film via the Layer-by-Layer Technique

Umaporn Paiphansiri, Pramuan Tangboriboonrat

Department of Chemistry, Faculty of Science, Mahidol University, 6 Rama Road, Phyathai, Bangkok 10400, Thailand

Received 11 August 2007; accepted 30 October 2008
DOI 10.1002/app.29464
Published online 13 January 2009 in Wiley InterScience (www.interscience.wiley.com).

ABSTRACT: An aqueous core containing a disinfectant agent (chlorhexidine digluconate) was encapsulated in a poly(methyl acrylate) shell with a modified nanoprecipitation technique. After redispersion of the capsules in an aqueous medium, the remaining amount of the disinfectant agent was as high as 90%. The nanocapsules were successfully adsorbed via the layer-by-layer technique onto a γ-radiation-vulcanized natural rubber latex sheet. Water contact angle measurements and scanning electron microscopy confirmed the presence of nanocapsules on the rubber surface. © 2009 Wiley Periodicals, Inc. J Appl Polym Sci 112: 769–777, 2009

Key words: core-shell polymers; morphology; rubber; self-assembly; surfaces

INTRODUCTION

The knowledge of natural rubber (NR) films is well evolved, especially for glove production, because the use of medical gloves is highly recommended for those individuals who are exposed to the blood or bodily fluids of patients. However, the problem of needle puncture or other accidents that might take place during surgery or patient treatment that could lead to viral infections of medical personnel needs to be addressed.[1–3] Busnel and coworkers[4,5] developed a medical glove that incorporates disinfectant droplets between its rubber sheets. When a needle punctures the glove, the disinfectant agent is released and neutralizes any infectious agents carried by the needle.

Among the several types of disinfectant agents, chlorhexidine digluconate (CHD) salt, a dicationic surfactant possessing a wide spectrum of activity against Gram-positive and Gram-negative bacteria, has been widely exploited.[6–8] To incorporate the water-soluble guest molecule, a well-defined nanocapsule with an aqueous core ideally has to be prepared in a single step, and the shell that is formed should be stable and have high structural perfection. However, the available protocols are still limited to water-in-oil (w/o) or inverse interfacial polymerization.[9–11] The inverse miniemulsion process, which generally provides critically stabilized small droplets dispersed in an organic continuous phase, has been applied. By the ultrasonication of a two-phase system, stable nanodroplets including the disinfectant agent for further encapsulation have been prepared by a modified nanoprecipitation method.[12–14] The droplet size, ranging from 30 to 500 nm, is principally governed by the type and amount of the surfactant used as the compatibilizer. One key characteristic of a miniemulsion is that no effective material exchange should occur between the droplets, and this is known as the Ostwald ripening effect.[15] In the case of an inverse miniemulsion, the salt or CHD (which is an extremely hydrophilic component) in aqueous miniemulsion droplets plays an important role in building up osmotic pressure inside each droplet.[13,16]

To physically adsorb polyelectrolytes, particles, or capsules onto a solid template, the layer-by-layer (LbL) technique, concerning mainly the sequential adsorption of oppositely charged materials via electrostatic attraction, is effectively used. A multilayer thin film with precise control of the structure and thickness at the molecular level has been fabricated via the LbL process.[17] Our previous works also showed that this method could be applied to inserting anionic polystyrene particles into a cationic polyelectrolyte assembled film coated on a glass substrate.[18,19] This effectively increased the film's

Correspondence to: P. Tangboriboonrat (scptb@mahidol.ac.th).

Contract grant sponsor: The Thailand Research Fund (to P.T.).
Contract grant sponsor: Royal Golden Jubilee (through its Ph.D. program to U.P.).
Contract grant sponsor: Deutscher Akademischer Austausch Dienst.

roughness and resulted in a significant increase in the hydrophobicity of the surface with Nafion at the outermost layer. Furthermore, the deposition of hard poly(methyl methacrylate) (PMMA) particles onto NR latex sheets successfully increased the surface roughness and hardness and hence diminished the friction of the rubber surface.[20,21]

Because the simple and versatile LbL process is independent of the substrate size and topology and does not affect the bulk properties of the substrate, it was used for the deposition of disinfectant nanocapsules onto γ-radiation-vulcanized natural rubber (RVNR) latex film, a medical glove model used in this study. The disinfectant nanocapsules were prepared by the modified nanoprecipitation of poly(methyl acrylate) (PMA) from an organic continuous phase onto w/o miniemulsion droplets containing the CHD solution. The effect of the concentration of PMA on the encapsulation efficiency of the nanocapsules was determined by proton nuclear magnetic resonance (^{1}H-NMR) measurements. After the redispersion of the nanocapsules into an aqueous medium, stable nanocapsules with high encapsulation efficiency were then selected to attach onto an RVNR latex sheet. Before the deposition of the soft disinfectant PMA nanocapsules onto the RVNR latex sheet, a study employing hard PMMA particles was performed as a function of the latex concentration and immersion time. The coated surface was then characterized by contact angle measurements, attenuated total reflection/Fourier transform infrared (ATR–FTIR) spectroscopy, and scanning electron microscopy (SEM).

EXPERIMENTAL

Materials

All chemicals, including CHD (20% in water; Sigma, Steinheim, Germany), potassium persulfate (KPS; Fluka, Germany), sodium dodecyl sulfate (SDS; Fluka, GC, Japan), soybean phosphatidylcholine (PC; Sigma), dichloromethane (Fluka, purum), cyclohexane (Fluka, purum), tetrahydrofuran (THF; Fluka; purum), ethanol (Fluka; purum), methanol (Fluka; purum), hexadecane (Fluka; purum), deuterated water, Nonidet (Biochemika, Fluka), pyrazine (Merck; GC, Japan), calcium chloride (Fluka, GR, Switzerland), and RVNR latex (Siam Okamoto Co., Ltd., Pathumthani, Thailand), were used without further purification. The monomers, methyl methacrylate (Fluka; purum, Deisenhafen, Germany) and methyl acrylate (Aldrich; 99%), were purified by passage through a column packed with neutral and basic aluminum oxide (Fluka; Purum). The block copolymer emulsifier poly[(butylene-*co*-ethylene)-*b*-(ethylene oxide)] [P(B/E-EO)], with a molecular mass of 3700 g/mol for the poly(butylene-*co*-ethylene) block and a molecular mass of 3600 g/mol for the poly(ethylene oxide) (PEO) block, was synthesized with Kraton liquid (Shell, TX).[22] PMA was prepared with the miniemulsion polymerization technique.[12,23]

Nanocapsule preparation

The organic continuous phase, comprising dichloromethane (9.5 g), a known amount of P(B/E-EO) or PC [% w/v: ratio of the surfactant (g) to the drug volume (mL)], and cyclohexane (12 g), was first prepared. An antiseptic agent, a CHD solution (0.5 mL), was charged into the solvent mixture. A solution of PMA (100 or 200 mg) in dichloromethane (0.5 g) was slowly dropped into the mixture, which was subsequently ultrasonicated for 2 min at 90% amplitude with a Branson W450 sonifier (Danbury, CT) with a 1/2″ tip. Then, the temperature was raised to 50°C in an open vessel with continuous mechanical stirring overnight. During the evaporation of dichloromethane, cyclohexane was added to replace dichloromethane and also its evaporated volume.

Characterization of the nanocapsules

The size of the nanocapsules was characterized with dynamic light scattering measurements (NanoZS, Malvern, UK). For the determination of the encapsulation degree of the antiseptic agent, the nanocapsules were separated by centrifugation in a microcentrifuge (Eppendorf) and were carefully dried before dissolution in a mixture of THF and ethanol. Deuterated water and a known amount of pyrazine were applied as an external solvent and as a calibration product for the quantitative analysis of the encapsulation efficiency by ^{1}H-NMR (DRX 400 with 400.123 MHz, Bruker).[24] The mass of the drug in the nanocapsule was calculated from the area ratio of the peaks at 7.66 and 9.07 ppm corresponding to aromatic protons of the CHD and pyrazine, respectively. The morphology of the capsules, which were mounted on a copper grid before coating with carbon, was investigated with transmission electron microscopy (TEM; EM 400, Phillips, Eindhoven, The Netherlands).

The separated nanocapsules were finally redispersed in a 2% (w/v) aqueous SDS solution with stirring overnight for complete deaggregation. The characterization procedures, mentioned previously, were also exploited, and the remaining amount of the drug in the nanocapsules after redispersion in water was evaluated.

Deposition of PMMA and/or disinfectant PMA nanocapsules onto an RVNR sheet

The dried rubber sheet (1.5 × 4 × 0.1 cm^3), cast from RVNR latex at room temperature, adhered to a poly(ethylene terephthalate) film without any adhesive. The rubber surface was cleaned by the immersion of the sample into distilled methanol (100 mL)

TABLE I
Characteristics of PMA Nanocapsules with 4% (w/v) P(B/E-EO) from Cyclohexane and a 2% (w/v) SDS Aqueous Solution

	Nanocapsules in cyclohexane [4% w/v P(B/E-EO)]		Redispersion nanocapsules [2% w/v SDS aqueous solution]	
PMA content (mg)	Size (nm)	Encapsulation efficiency (%)	Size (nm)	Remaining disinfectant agent (%)
100	150	100	456	87
200	190	100	258	85

and then Milli-Q water (100 mL) for 15 min for each step during sonication in an ultrasonic cleaning bath. After drying in air, the obtained rubber sheet was kept in a desiccator.

PMMA latex was synthesized by miniemulsion polymerization.[24] An aqueous solution of Nonidet (1–8 wt % dry latex) was then added to PMMA latex [1% total solid content (TSC)] before shaking (Burell) for 12 h at room temperature. The amount of Nonidet adsorbed onto the particles was deduced from the quantity of an aqueous solution of 0.5*M* $CaCl_2$ added to provoke visible coagula.

PMMA (Nonidet) was prepared by the addition of an 8 wt % concentration of the dry latex to PMMA latex having TSCs of 0.1, 0.5, and 0.85%. The RVNR strip was then immersed into the PMMA (Nonidet) latex at pH 2 for various time intervals. The sample was subsequently washed with water via a series of three rinsing baths and finally dried at room temperature. The optimum condition of PMMA adsorption was further applied for the incorporation of a 0.85% TSC of disinfectant PMA nanocapsules.

Surface analysis of PMMA (Nonidet) and/or disinfectant PMA nanocapsules (Nonidet) deposited onto an RVNR sheet

The surface of PMMA deposited onto an RVNR sheet was characterized with ATR–FTIR spectroscopy (Equinox 55, Bruker). The spectra (32 scans at a 4-cm^{-1} resolution) were collected with a Ge crystal in a multireflection mode. The change in the characteristic absorption peaks at 1730 and 1378 cm^{-1}, corresponding to C=O stretching of the carboxylate group of PMMA and C—H bending of —CH_3 of NR, respectively, was investigated.

A sessile drop contact angle measurement was performed on RVNR adsorbed with disinfectant PMA nanocapsules with a contact angle goniometer (G-1, Kruss, Hamburg, Germany). The surface morphology of the modified RVNR sheet was determined by SEM (JSM 5410LV, JEOL, Tokyo, Japan).

RESULTS AND DISCUSSION

PMA nanocapsules

The characterization of PMA nanocapsules with 4% (w/v) P(B/E-EO) dispersed in cyclohexane and redispersed in a 2% (w/v) SDS aqueous solution was carried out, and the data are listed in Table I.

It was observed that the nanocapsule sizes were 150 and 190 nm with 100 and 200 mg of PMA, respectively. An encapsulation efficiency of 100% with both concentrations was detected by ^{1}H-NMR measurement. After redispersion of the PMA nanocapsules, the remaining amount of the disinfectant agent was as high as about 90%. The dissolution of a large amount of PMA (300–500 mg) in the continuous phase took more time in comparison with other polymers.[24] The high viscosity of the PMA solution caused the formation of coagulum during the evaporation of dichloromethane; consequently, probably because of the low mobility of the molecular chains, the polymer did not deposit onto the aqueous nanodroplets.[25]

Besides P(B/E-EO), the other surfactant used for the preparation of PMA nanocapsules was PC, a double-tailed zwitterionic surfactant, the chemical structure of which is shown in Figure 1. With a disinfectant agent volume of 0.5 mL and a solvent mixture volume of 22 mL and with a dichloromethane/cyclohexane ratio of 1 : 1.2, the optimum formulation of the inverse miniemulsion for the nanocapsule preparation was limited to 150 mg of PMA and 100 mg of PC (or 20% w/v with respect to the disinfectant volume).

As previously mentioned, the size of the aqueous miniemulsion droplets dispersed in the cyclohexane phase can be designed by the type and amount of the surfactant applied. In comparison with 4% (w/v) P(B/E-EO), a PC content as high as 20% (w/v) was required to obtain stable disinfectant nanodroplets, which were dispersed in a solvent mixture of dichloromethane and cyclohexane containing PMA. This might be explained in term of self-assembly characteristic of PC molecules on the nanodroplet surface.[26] Yamada et al.[27] proposed that a well-defined trilayer membrane of PC with an 8-nm

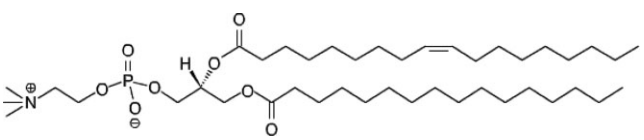

Figure 1 Chemical structure of soybean PC.

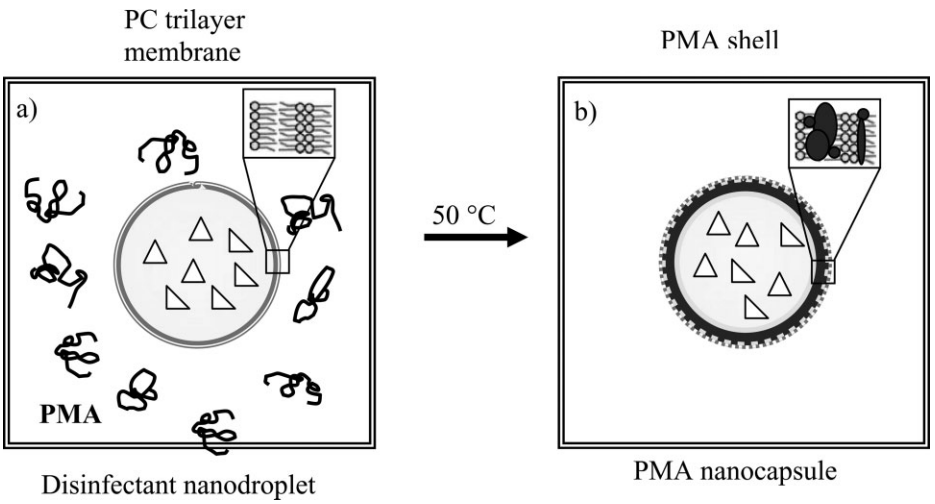

Figure 2 Schematic representation of (a) a PC-stabilized disinfectant nanodroplet in a solvent mixture of dichloromethane and cyclohexane and (b) a PMA nanocapsule dispersed in a cyclohexane phase.

thickness, organized spontaneously on a water nanodroplet, was responsible for steric stabilization in an organic continuous phase, as depicted in Figure 2(a). The internal membrane structure was constructed from the alternative orientation of each self-assembled PC layer: the first and third layers turned their hydrophilic head groups toward the nanodroplet and exposed hydrophobic alkyl chains of the third layer to the organic phase. The second layer intervened, placing alkyl chains with those of the first layer, and the head group encountered the head group of the third layer.[27] In the presence of PC's trilayer membrane, the precipitated PMA was possibly deposited onto the hydrophobic tails of PC's outermost layer or inserted within the hydrophobic part of the assembled membrane, as schematically displayed in Figure 2(b). Consequently, PMA nanocapsules about 306 nm in diameter, dispersed in the cyclohexane phase, were obtained.

After the separation of PMA nanocapsules from the cyclohexane phase by centrifugation, the nanocapsules could spontaneously redisperse into the water phase without the addition of any surfactant under continuous stirring overnight. This might be due to the reorientation of the top PC layer by the turning of its hydrophilic head group toward the aqueous continuous phase and/or migration of the PC molecules in the second layer to the nanocapsule surface so that the PMA nanocapsule would gain electrostatic stabilization.[27,28] The stable aqueous core nanocapsule dispersed in water, having an average size of 216 nm, was hence evaluated. The ζ-potential of the PMA nanocapsule against the pH was then monitored, as shown in Figure 3.

The results indicated that the PMA nanocapsule exhibited positive character when the pH was below 9.4. Above this pH, the ζ-potential was negative. This amphoteric character, having a pI of 9.4, confirmed the presence of choline [$N(CH_3)_3$] and phosphate moieties of PC, which imparted particle stability, on the nanocapsule surface. Our results agreed well with a former work[29] concerning the utilization of poly[2-(methacryloyloxy)ethyl phosphorylcholine]-*block*-poly[2-(dimethylamino)ethyl methacrylate] for stabilizing gold nanoparticles in an aqueous phase.

Morphological study of the PMA nanocapsules

TEM micrographs of air-dried nanocapsules using 100 mg of PMA with 4% (w/v) P(B/E-EO) from the cyclohexane phase were previously displayed.[25] It was observed that the size of the nanocapsules was remarkably smaller than that obtained from the dynamic light scattering measurements because the nanocapsules greatly shrank under the high-energy electron beam in TEM. However, the core–shell morphology of the nanocapsules could be clearly noted.

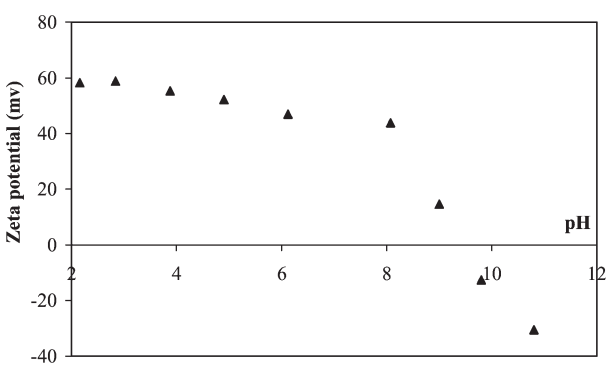

Figure 3 ζ-Potential of PMA nanocapsules prepared with 150 mg of PMA and 20% (w/v) PC versus the pH.

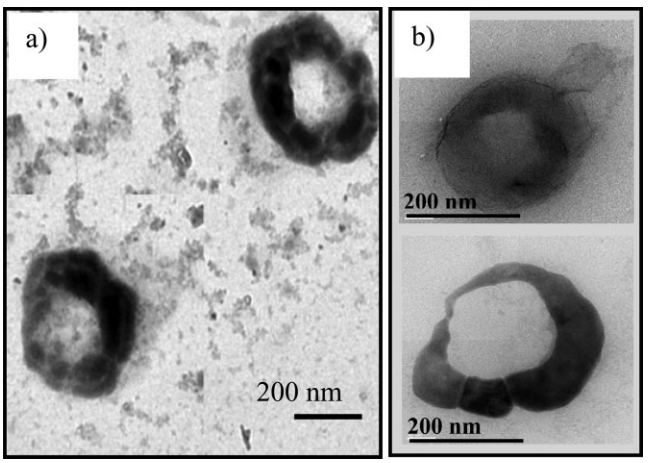

Figure 4 TEM micrographs of nanocapsules with 150 mg of PMA and 20% (w/v) PC: (a) dispersed in cyclohexane and (b) redispersed in an aqueous phase.

The morphologies of PMA nanocapsules (with 150 mg of PMA and 20% w/v PC) dispersed in cyclohexane and redispersed in an aqueous phase were evaluated, and the TEM micrographs are shown in Figure 4.

It was observed that the PMA nanocapsules possessed a spherical shape with a core–shell morphology in both cyclohexane and after redispersion into the aqueous phase. However, the PMA shell was denser than that prepared with 4% (w/v) P(B/EEO).[24] This might be due to the fact that the PC trilayer, organizing on the disinfectant nanodroplet surface, contributed to hydrophobic vacancy. A large amount of precipitated PMA was entrapped, and this gave rise to the formation of the thick shell. The disinfectant PMA nanocapsule, prepared with 20% (w/v) PC, was used for incorporation into an RVNR latex sheet in further steps.

Deposition of PMMA latex particles onto an RVNR latex sheet

Monodisperse PMMA latex with an average size of 143 ± 0.5 nm and a TSC of 20.3 ± 0.03% was attained. The ζ-potentials at pH 2–11 were negative, and this was possibly derived from the strong acidic groups (SO_4^-) from KPS and SDS, which served as the initiator and anionic surfactant, respectively.

To determine the change from electrostatic stabilization to steric stabilization of the PMMA latex adsorbed with a nonionic surfactant, Nonidet, whose molecule contains PEO moieties, an electrolyte solution was added to provoke the visible coagula. The results showed that the volume of 0.5*M* $CaCl_2$ required for PMMA latex coagulation was increased with increasing Nonidet concentration. With less than 8% Nonidet, PMMA latex was immediately coagulated after the addition of a $CaCl_2$ aqueous solution. On the contrary, the latex remained stable at a minimum Nonidet concentration of 8%. The modification of latex stabilization from electrostatic stabilization to steric stabilization was, therefore, achieved with 8% Nonidet.

Because an LbL hydrogen-bonded film can be generated by the self-assembly of a weak polyacid and a neutral polymer at a low pH, the study of deposition of PMMA adsorbed by Nonidet [PMMA (Nonidet)] onto an RVNR latex sheet at pH 2 proceeded. The presence of PMMA (Nonidet) deposited onto an RVNR latex sheet with various immersion times at latex concentrations of 0.1, 0.5, and 0.85% was elucidated with ATR–FTIR. The spectra of RVNR sheets dipped into 0.1% PMMA (Nonidet) at different times are illustrated in Figure 5.

In the spectrum of RVNR, the characteristic peaks at 2961, 2922, and 2856 (C—H stretching), 1450 (C—H bending of —CH_2—), 1378 (C—H bending of —CH_3), and 837 cm^{-1} (C—H deformation of *cis* C=C—H) were detected. After the deposition of PMMA (Nonidet), an additional peak, a strong absorption at 1730 cm^{-1} related to C=O stretching of the carboxylate group, was observed. In addition, the intensity of the latter increased with increasing immersion time; concomitantly, the intensity of the absorbance at 1378 cm^{-1} of RVNR decreased. This implied an interpolymer complex formation between PEO groups on the PMMA surface and carboxylic

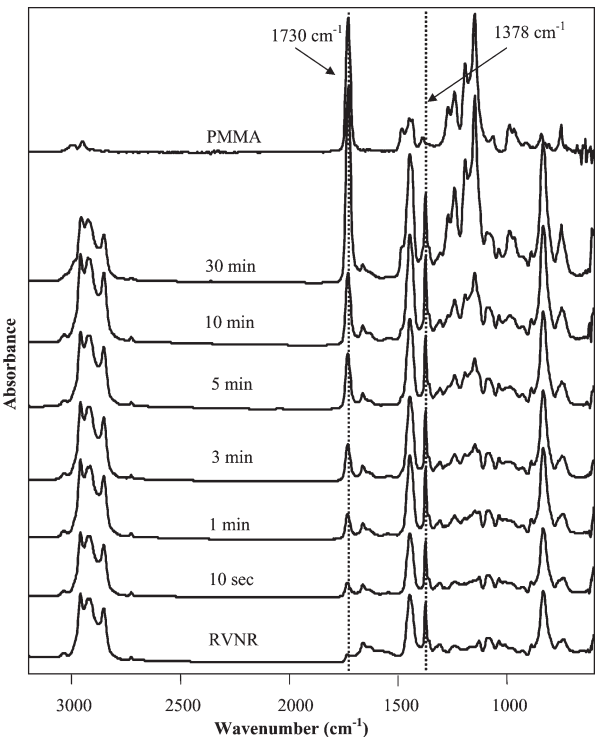

Figure 5 ATR–FTIR spectra of RVNR latex sheets immersed in 0.1% PMMA (Nonidet; pH 2) at various dipping times.

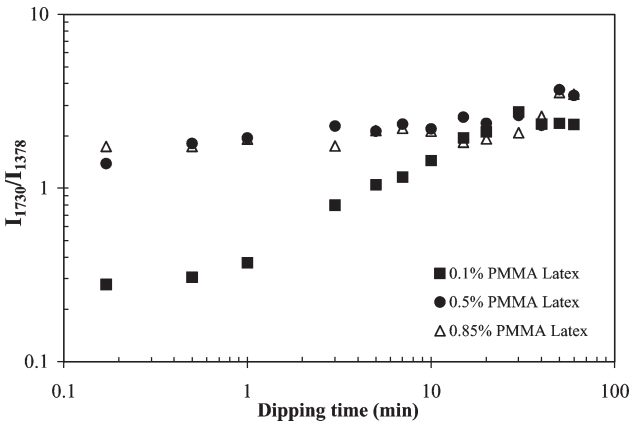

Figure 6 Absorbance ratios of 1730- and 1378-cm^{-1} peaks (I_{1730}/I_{1378}) for RVNR sheets deposited with PMMA latex (0.1, 0.5, or 0.85%) as a function of the dipping time.

groups of the residual protein substance on RVNR, which played a role in the driving force for PMMA deposition.[30,31]

To evaluate the change in the PMMA (Nonidet) content on the RVNR sheet, the absorbance ratios of the peak at 1730 cm^{-1} of PMMA to that at 1378 cm^{-1} of RVNR were calculated and plotted versus the dipping times at latex concentrations of 0.1, 0.5, and 0.85%, as depicted in Figure 6.

The results indicated that at the low latex concentration of 0.1%, the adsorption was directly proportional to the immersion time of 1–30 min and then approached a constant value after 30 min. At high latex concentrations of 0.5 and 0.85%, the deposition contents were almost constant within 1 min. Our results were in agreement with the former work, which reported that the repulsion among latex

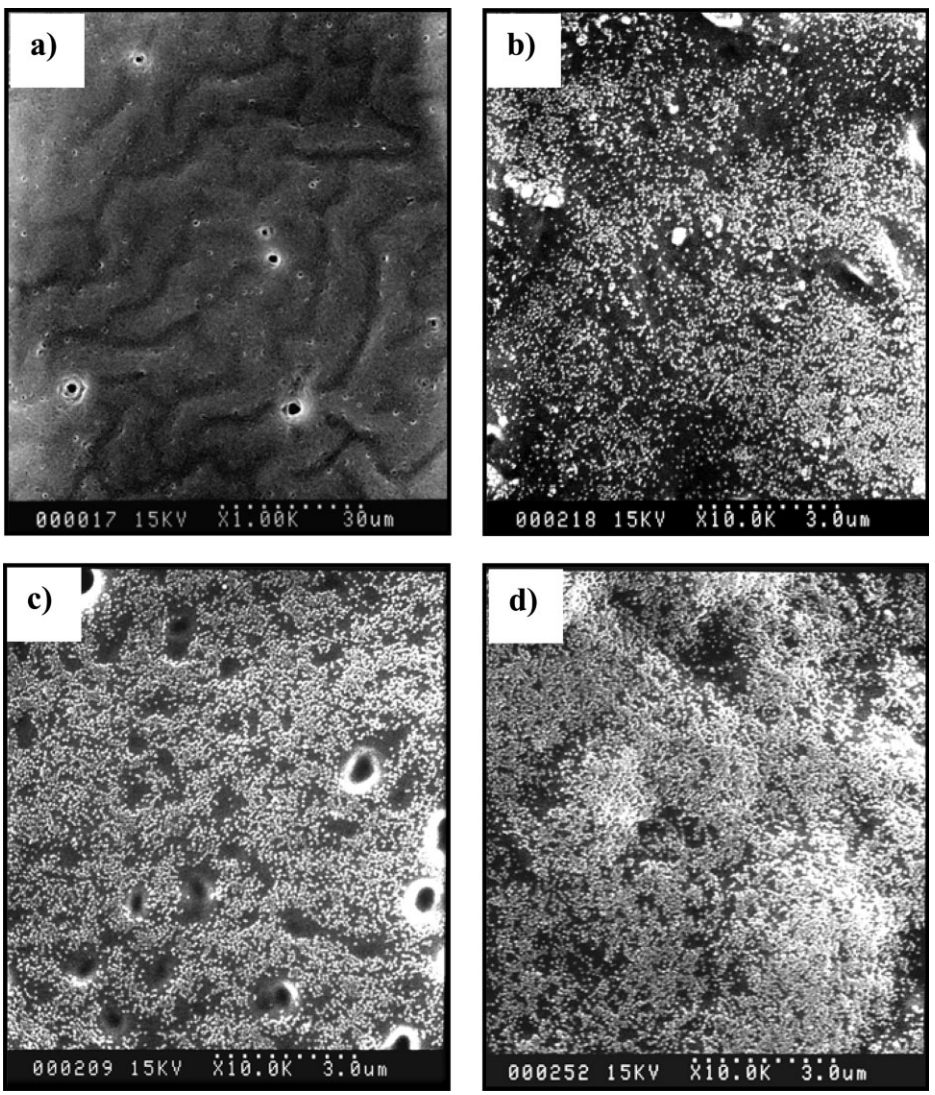

Figure 7 SEM micrographs of (a) pristine RVNR and (b–d) RVNR adsorbed with 0.1% PMMA (Nonidet) as a function of the dipping time (10 s, 1 min, and 30 min, respectively).

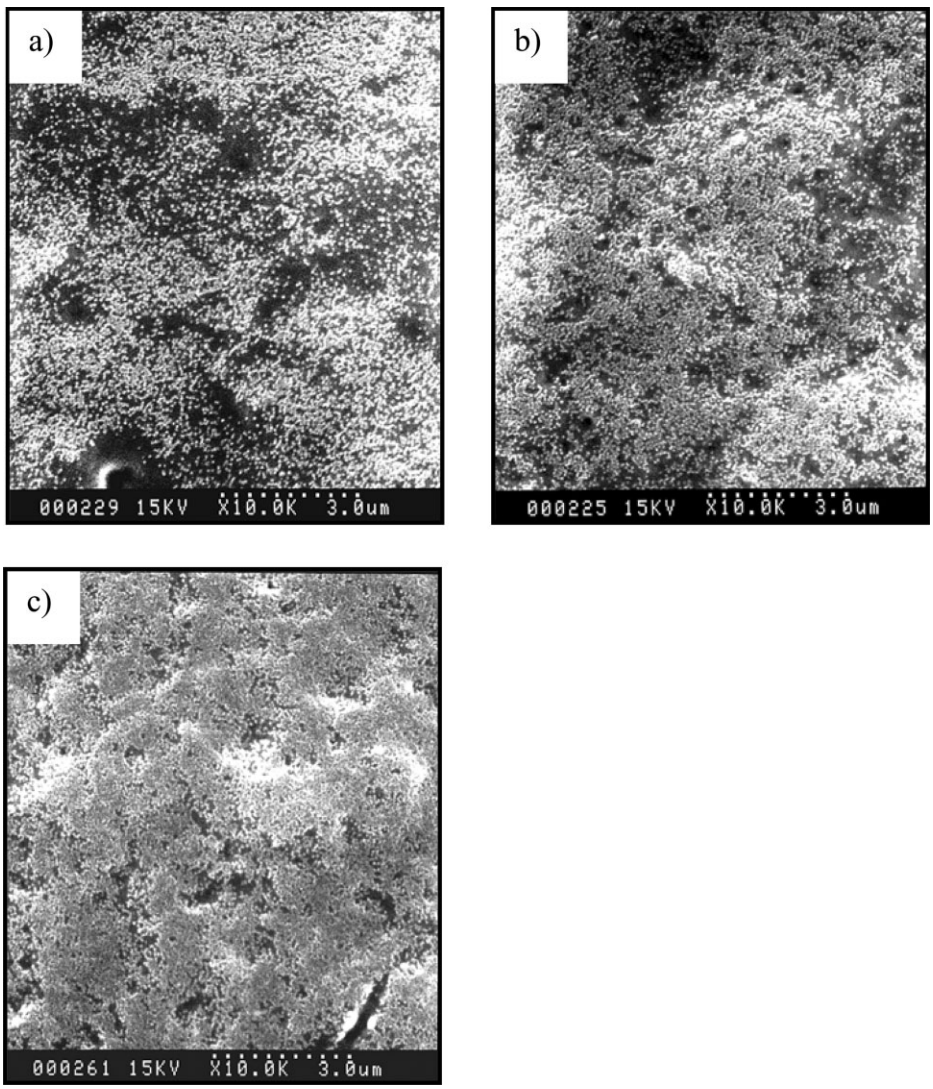

Figure 8 SEM micrographs of RVNR adsorbed with 0.85% PMMA (Nonidet) as a function of the dipping time: (a) 10 s, (b) 30 s, and (c) 30 min.

particles at high latex concentrations provided a high collision between the particles and substrate surface.[18–21] Because the adsorption rate and surface coverage depended strongly on the size of the colloidal particle,[32] the small size of PMMA, containing more active sites to attract the substrate surface, was therefore attributed to comparable deposition contents at all latex concentrations after 30 min of dipping.

The morphologies of RVNR sheets coated with PMMA (Nonidet) at different dipping times were investigated with SEM. The micrographs for 0.1 and 0.85% PMMA (Nonidet) are displayed in Figures 7 and 8, respectively.

It was noted that the pristine RVNR surface in Figure 7(a) exhibited a curvature with several voids, which might be attributed to the detachment of additives applied in the commercial latex. With the increasing immersion time of PMMA (Nonidet), as shown in Figures 7(b–d) and 8(a–c), dense particles packed onto the rubber surface were more pronounced. In comparison with the high latex concentration of 0.85% presented in Figure 8, relatively closed packing of the particles could be obtained with 30 s of dipping, as shown in Figure 8(b). Furthermore, the multilayer particles deposited onto the substrate at the immersion time of 30 min are revealed in Figure 8(c), and they might be due to the bridging formation of free latex particles that collided with the particles occupied on the rubber surface.[33,34]

Deposition of disinfectant PMA nanocapsules (Nonidet) onto an RVNR latex sheet

From the success of PMMA (Nonidet) deposition, a 0.85% TSC of PMA nanocapsules prepared with 20% (w/v) PC was adsorbed with 8% Nonidet before deposition onto RVNR at pH 2. Because the

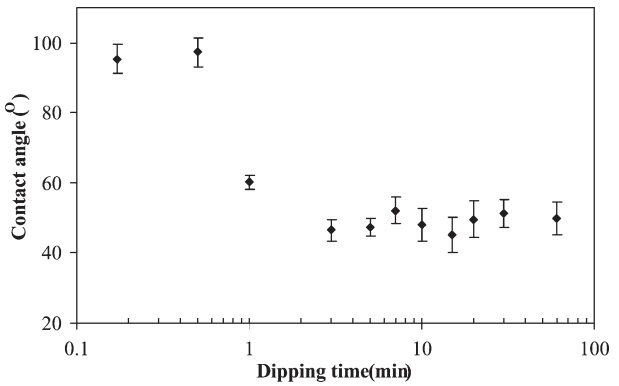

Figure 9 Water contact angle of a PMA nanocapsule (Nonidet) deposited onto an RVNR sheet as a function of the dipping time.

existence of polar groups could lower the hydrophobicity of the substrate, the water contact angle of the PMA nanocapsule (Nonidet) deposited onto an RVNR sheet as a function of the dipping time was measured. The data are presented in Figure 9.

The results indicated that the contact angles rapidly decreased from 95 ± 4 to 46 ± 2° with the immersion time of 3 min and then remained constant. The low contact angle confirmed the presence of nanocapsules, whose surface bore PC and/or Nonidet molecules, on the rubber surface. Our results agreed well with a previous work,[35] which reported that the grafting of phosphorylcholine onto a poly(ether urethane) surface exhibited a water contact angle of 43°. The insignificant change when the dipping time was greater than 3 min might be due to the limitation of the technique; that is, the contact angle measurement is sensitive only for the analysis of the outermost surface.[36] Thus, the increment of the deposition amount of the nanocapsules with increasing deposition time would not affect the contact angle.

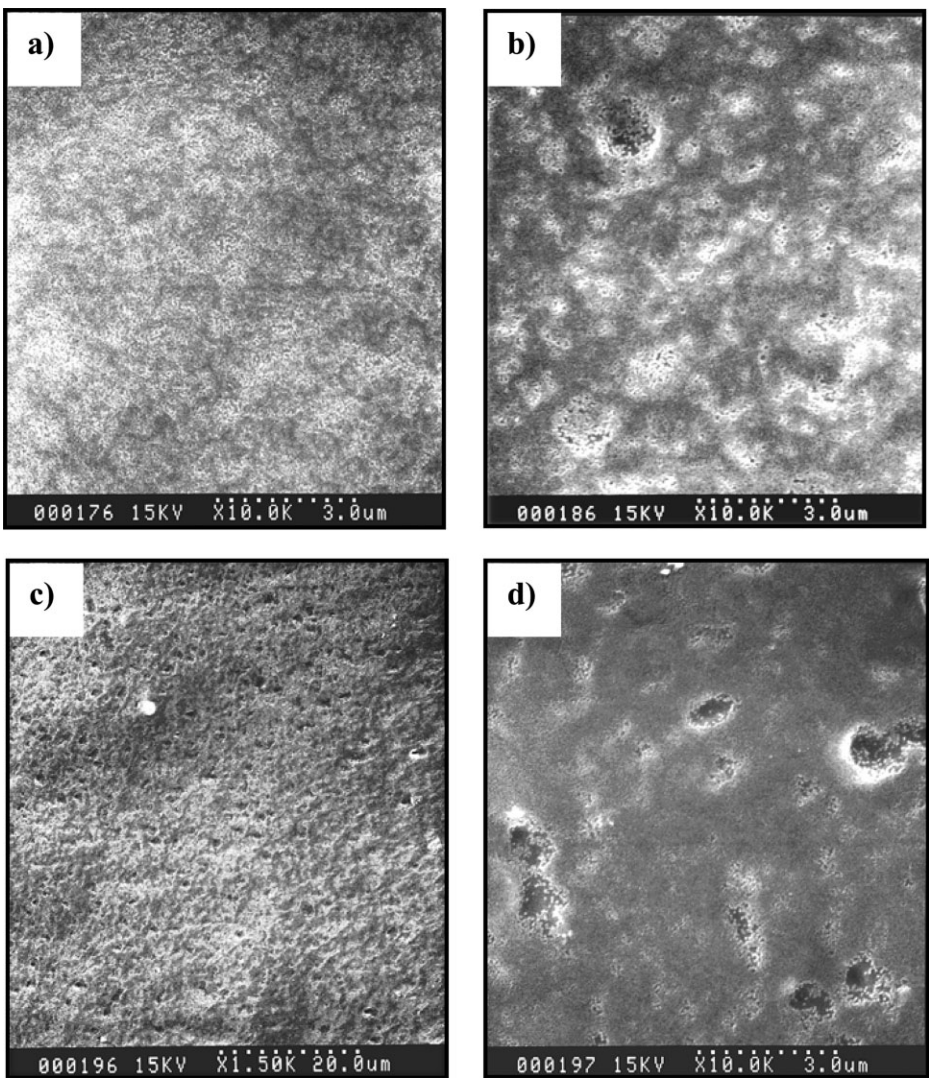

Figure 10 SEM micrographs of a PMA nanocapsule (Nonidet) deposited onto an RVNR sheet as a function of the dipping time: (a) 10, (b) 30, and (c,d) 50 min.

The surface morphologies of PMA nanocapsules (Nonidet) deposited onto rubber sheets with various dipping times were determined, and the SEM micrographs are illustrated in Figure 10. The rubber surface appeared smoother with the dipping time increasing from 10 to 50 min. The explanation was that PMA with a low glass-transition temperature formed a film at room temperature and hence covered the curvature and large voids on the pristine RVNR surface. It could therefore be assumed that the incorporation of disinfectant PMA nanocapsules into the RVNR latex sheet was achieved through the formation of an interpolymer complex driven at pH 2 as previously mentioned.

CONCLUSIONS

The formation of aqueous core nanocapsules by controlled polymer nanoprecipitation onto inverse miniemulsion droplets containing CHD has been conclusively established. The deposition of a PMA shell from an organic continuous phase onto a dispersed phase of stable nanodroplets was achieved by changes in the gradient of the solvent/nonsolvent mixture of dichloromethane and cyclohexane under mild evaporation. After the redispersion of the nanocapsules in an aqueous medium, stable nanocapsules with an aqueous core redispersed in the aqueous continuous phase were obtained. The success of the deposition of PMMA latex particles on an RVNR sheet via the LbL technique led to the development of PMA nanocapsules adsorbed onto the rubber film. The low contact angle confirmed the presence of nanocapsules, whose surface bore PC and/or Nonidet molecules, on the RVNR surface. The surface morphologies of PMA nanocapsules (Nonidet) deposited onto the rubber sheet with various dipping times were observed by SEM.

References

1. Eklund, A. M.; Ojajärvi, J.; Laitinen, K.; Valtonen, M.; Werkkala, K. A. Ann Thorac Surg 2002, 74, 149.
2. Osman, M. O.; Jensen, S. L. World J Surg 1999, 23, 630.
3. Yazdanpanah, Y.; Boelle, P. Y.; Carrat, F.; Guiguet, M.; Abiteboul, D.; Valleron, A. J. J Hepatol 1999, 30, 765.
4. Busnel, R. G.; Argy, G. U.S. Pat. 5,024,852 (1991).
5. Busnel, R. G.; Cheymol, A.; Riess, G. U.S. Pat. 5,804,628 (1998).
6. Mulberry, G.; Snyder, A. T.; Heilman, J.; Pyrek, J.; Stahl, J. Am J Infect Control 2001, 29, 377.
7. Lboutounne, H.; Chaulet, J. F.; Ploton, C.; Falson, F.; Pirot, F. J Controlled Release 2002, 82, 319.
8. Lafforgue, C.; Carret, L.; Falson, F.; Reverdy, M. E.; Freney, J. Int J Pharm 1997, 147, 243.
9. Pitaksuteepong, T.; Davies, N. M.; Tucker, I. G.; Rades, T. Eur J Pharm Biopharm 2002, 53, 335.
10. Watnasirichaikul, S.; Rades, T.; Tucker, I. G.; Davies, N. M. Int J Pharm 2002, 235, 237.
11. Wu, D.; Scott, C.; Ho, C. C.; Co, C. C. Macromolecules 2006, 39, 5848.
12. Landfester, K.; Bechthold, N.; Tiarks, F.; Antonietti, M. Macromolecules 1999, 32, 5222.
13. Landfester, K.; Willert, M.; Antonietti, M. Macromolecules 2000, 33, 2370.
14. Landfester, K.; Bechthold, N.; Tiarks, F.; Antonietti, M. Macromolecules 1999, 32, 2679.
15. Sudol, E. D.; El-Aasser, M. S. In Emulsion Polymerization and Emulsion Polymers; Lovell, P. A.; El-Aasser, M. S., Eds.; Wiley: Chichester, UK, 1997.
16. Landfester, K. Adv Mater 2001, 13, 765.
17. Decher, G. Science 1997, 277, 1232.
18. Sangribsub, S.; Tangboriboonrat, P.; Pith, T.; Decher, G. Polym Bull 2005, 53, 425.
19. Sangribsub, S.; Tangboriboonrat, P.; Pith, T.; Decher, G. Eur Polym J 2005, 41, 1531.
20. Sruanganurak, A.; Sanguansap, K.; Tangboriboonrat, P. Colloid Surf A 2006, 289, 110.
21. Sruanganurak, A.; Tangboriboonrat, P. Colloid Surf A 2007, 301, 147.
22. Schlaad, H.; Kukula, H.; Rudloff, J.; Below, I. Macromolecules 2001, 34, 4302.
23. Bechthold, N.; Landfester, K. Macromolecules 2002, 33, 4682.
24. Paiphansiri, U.; Tangboriboonrat, P.; Landfester, K. Macromol Biosci 2006, 6, 33.
25. Caruso, F. Colloids and Colloid Assemblies; Wiley-VCH: Weinheim, 2004.
26. Gupta, R.; Muralidhara, H. S.; Davies, H. T. Langmuir 2001, 17, 5176.
27. Yamada, A.; Yamanaka, T.; Hamada, T.; Hase, M.; Yoshikawa, K.; Baigl, D. Langmuir 2006, 22, 9824.
28. Schrader, W.; Kaatze, U. J Phys Chem B 2001, 105, 6266.
29. Yuan, J.-J.; Schmid, A.; Armes, S. P. Langmuir 2006, 22, 11022.
30. DeLongchamp, D. M.; Hammond, P. T. Langmuir 2004, 20, 5403.
31. Tangboriboonrat, P.; Buranabunya, U. Colloid Polym Sci 2001, 279, 615.
32. Litton, G. M.; Olson, T. M. Colloid Surf A 1996, 107, 273.
33. Zhang, L.; Liu, Y.; Liu, Z. J Appl Polym Sci 1993, 49, 1415.
34. Elimelech, M. Particle Deposition and Aggregation: Measurement, Modeling and Simulation; Colloid and Surface Engineering Series; Butterworth-Heinemann: Woburn, MA, 1995.
35. Van der Heiden, A. P.; Willems, G. M.; Lindhout, T.; Pijpers, A. P.; Koole, L. H. J Biomed Res 1998, 40, 195.
36. Castell, P.; Wouters, M.; de With, G.; Fischer, H.; Huijs, F. J Appl Polym Sci 2004, 92, 2341.